Volume 15 Number 19 1987 Nucleic Acids Research

An abasic site in DNA. Solution conformation determined by proton NMR and molecular mechanics calculations

Ph.Cuniasse, L.C.Sowers[1], R.Eritja[2], B.Kaplan[2], M.F.Goodman[1], J.A.H.Cognet[3], M.LeBret[3], W.Guschlbauer and G.V.Fazakerley

Service de Biochimie, Bat.142, Département de Biologie, Centre d'Etudes Nucléaire de Saclay, F-91191 Gif-sur-Yvette Cédex, France, [1]Molecular Biology Section, Department of Biological Sciences, University of Southern California, Los Angeles, CA 90089-1481 and [2]Department of Molecular Genetics, Beckman Research Institute of City of Hope, Duarte, CA 91010, USA

Received July 21, 1987; Revised and Accepted September 7, 1987

ABSTRACT

We have determined the three-dimensional structure of a non-selfcomplementary nonanucleotide duplex which contains an abasic (apyrimidinic) site in the centre, i.e. a deoxyribose residue opposite an adenosine. The majority of the base and sugar proton resonances were assigned by NOESY, COSY and 2DQF spectra in D_2O and H_2O. We have measured the initial slope of buildup of NOEs in NOESY spectra at very short mixing times (25 to 50 ms), and from these were able to establish interproton distances for the central part of the duplex. We propose a different strategy for proton-proton distance determinations which takes into account the observed variations in correlation times for particular proton-proton vectors. A set of 31 measured interproton distances was incorporated into the refinement of the oligonucleotide structure by molecular mechanics calculations. Two structures were obtained which retain all aspects of a classical B DNA in which the unpaired adenine and the abasic deoxyribose lie inside the helix. We observe that the non-hydrogen bonded adenine is held well in the helix, the Tm of this base being the same as that of the A•T base pairs in the same duplex.

INTRODUCTION

Apurinic or apyrimidinic (abasic) sites are the most frequent damage encountered in DNA (1,2). These non coding lesions arise through cleavage of the glycosidic bond by spontaneous hydrolysis (1,2) and further, the rate of cleavage may be significantly accelerated by DNA modification. The glycosidic bonds of many modified bases, particularly purines, undergo spontaneous hydrolysis at very high rates under physiological conditions (3). In addition to hydrolysis many chemically or radiation damaged bases are removed from DNA most often arise from enzymatic removal of uracil residues in DNA (5). Uracil residues in DNA result from either incorporation of dUTP or deamination of cytosine residues (6). Repair of abasic sites in DNA is initiated by AP endonuclease (7).

If unrepaired, the presence of an abasic site on a DNA template creates a significant challenge for DNA polymerase. Most frequently in vitro, chain elongation is inhibited (8,9). If elongation occurs, it is unli-

kely that the correct base will be incorporated because the coding information has been lost. Previous studies have shown that incorporation can occur opposite abasic sites at reduced rates, and A is incorporated most often, followed by G (9-12). The preference for nucleotide insertion exhibited by DNA polymerase at the abasic site is as yet unexplained. The relative stability of oligonucleotides derived from melting temperatures (13), is inconsistant with observed enzyme preferences (9-12). Further, recent data presented by Randall et al. (12) indicate that differences in insertion frequency by DNA polymerase are primarily due to Vmax, and not Km differences, suggesting that geometric, rather than thermodynamic factors may be responsible for the preferred incorporation of A at abasic sites.

Due to the importance of abasic sites as mutagenic intermediates in vivo, we have investigated the structure of an oligonucleotide containing an abasic lesion. Because A is the substrate favoured by DNA polymerase for insertion opposite the abasic site, we have investigated both the structure and dynamics of a non self complementary nonanucleotide containing A opposite an abasic site by 1D and 2D NMR techniques. In order to determine the conformation of the oligonucleotide, inter proton distances determined by NMR were incorporated into the refinement of the structure by molecular mechanics calculations. Two models that satisfy the distance constraints are presented.

MATERIALS AND METHODS

The two nonanucleotides were synthetized by a classical phosphotriester method (14,15). They were anealed to form the duplex:

$5'(C^1\ G^2\ T^3\ G^4\ dr^5\ G^6\ T^7\ G^8\ C^9)3'$

$3'(G^{18}\ C^{17}\ A^{16}\ C^{15}\ A^{14}\ C^{13}\ A^{12}\ C^{11}\ G^{10})5'$

The duplex was 4 mM in strand, dissolved in 10 mM phosphate buffer, 150 mM NaCl and 0.2 mM EDTA. NMR spectra were recorded in either 99.99% D_2O or 90% H_2O/10% D_2O. Chemical shifts were measured relative to internal tetramethylammonium chloride (3.18 ppm).

NMR spectra

The spetra did not change over the ca.6 months during which measurements were made. This abasic site is chemically stable.

NMR spectra were recorded on a Bruker WM500 spectrometer. NOESY spectra with different mixing times (25, 35, 50, 100, 300 ms) were recorded in the phase sensitive mode (16) with 2K data points in the t_1 dimension and 125 acquisitions per spectrum. 250 free induction decays were collected in

the t_2 dimension. After zero filling to give a 2K x 2K matrix, a sine bell (shifted by $\pi/2$ for cross peak volume determination) was applied to the data in both dimensions prior to Fourier transformation.

The COSY spectrum was obtained using a $\pi/4$-t-$\pi/4$ sequence and the data treated as above.

The double quantum spectrum in D_2O was recorded in the absorption mode (17).

A $3(\pi/2$-t-$\pi/2)$ hard pulse sequence with a 200 ms mixing time was used to record the NOESY in H_2O in the absorption mode (18). The rate of imino exchange with solvent was measured by a technique described recently.(19)

Molecular mechanics calculations.

Energy minimizations were carried out using the program AMBER (20) on a VAX 8600 computer. The parameters were those describe by Weiner et al. (21). All hydrogen atoms are treated explicitly. To simulate screening effects of the solvent, a gas phase potential was employed where the electric constant is proportional to the distance r_{ij} separating a pair of atoms: $D_{ij}=C*r_{ij}$ (22). The proportionality constant C was taken as 4 A^{-1}. Refinement was terminated when the norm of the energy gradient was less than 0.05 kcal/A. The negative charge of the phosphate groups of the oligonucleotide were neutralized by spheres with a positive unit charge and were originally set at 3 A from the phosphate oxygen atoms by the subprogram EDIT of AMBER. When thicker spheres were used and set at 6.7 A away from the phosphate oxygen atom, the energy was lowered by 11%, that is about 80 kcal, but the local geometry of the oligonucleotide was not altered.

In order to incorporate NMR distance data into the computational refinement of the oligonucleotide structure, the following procedure was used. The distance separating the protons listed in Table II, found to be d_{ij} in the simulation of the structure, were constrained to the NMR values r_{ij} with the penalty function, $E= \Sigma K(d_{ij}-r_{ij})^2$. The penalty constant,K, was set equal to 500 kcal/(mol*A^2) in the first refinement. Then K was progressively decreased in five subsequent refinements, taking the values 100, 50, 5, 1, 0 kcal/(mol*A^2). This constrained energy minimization procedure was found to depend on the starting oligonucleotide structures. As the NMR data indicated that the oligomer structure had B DNA features, the minimization was started from various conformations, all derived from the fibre structure of Arnott et al. (23). Among the structures obtained, only the best two were retained.

In model 1, the starting conformation of the oligonucleotide was

that of Arnott et al. (23). A single constrained energy minimization procedure yielded structure S1. In model 2, the oligonucleotide d(CGTGTGTGC)•d(GCACACACG) was generated as the B structure of Arnott et al. (23). Its structure was refined through energy minimization ignoring the NMR data. This yielded structure S0. Then the thymine was replaced by a proton. After inclusion of the NMR data, the constrained energy minimization procedure was then iterated 13 times, up to convergence, the resulting structure of one iteration being the starting structure of the next one. During each iteration of the procedure the penalty constant took the values 500, 100, 50, 5, 1, 0 kcal/(mol•A^2) sucessively. The limit structure obtained after convergence is S2.

The molecular structures were displayed on a raster monitor LEX 90 using the program NACAD, developped by J. Gabarro and M. Le Bret (to be published).

RESULTS

NOESY in H_2O: assignement of imino and amino protons.

The 1D 500 MHz NMR spectrum in 90%H_2O at 1°C is shown in Fig. 1. The imino protons are observed in the low field region, between 12 and 14 ppm, while the region between 8.6 and 5.3 ppm contains the WC and NWC protons of cytidine residues, the H6 and H8 base protons and the H2 adenosine protons.

We have recorded a NOESY spectrum in H_2O at 1°C to establish the connectivities between the imino, H2 and amino protons of the different base pairs. An expanded contour plot of the imino and base proton region is shown in Fig. 2. The diagonal corresponds to the one dimensional spectrum. Each connectivity between two protons gives a cross peak off diagonal. In the low

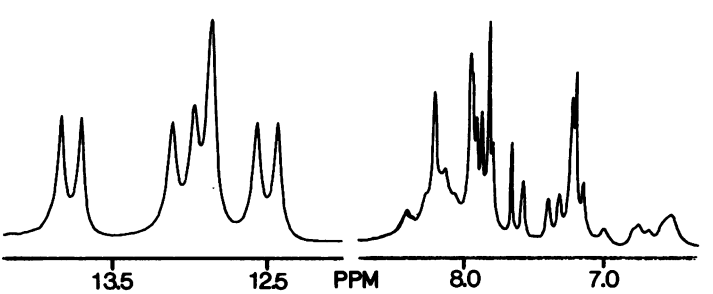

Fig. 1: Imino and aromatic region of the NMR spectrum of the duplex at 1°C in 90% H_2O (the scale is not the same for the two regions).

field region between 13.5 and 14 ppm we observe the two T imino protons, each giving as expected one intense cross peak in the aromatic region corresponding to the connectivity with the AH2 of the A•T base pair. In the region between 12.3 and 13.3 ppm we find the G imino protons. Two of them, at 12.99 and 13.13 ppm, when compared with the 1D spectrum are strongly reduced in intensity by the 2D pulse sequence. Each of the two G imino resonances at highest field (12.44 and 12.58 ppm) show four cross peaks in the aromatic region. Two of these are with exchangeable proton resonances and must arise

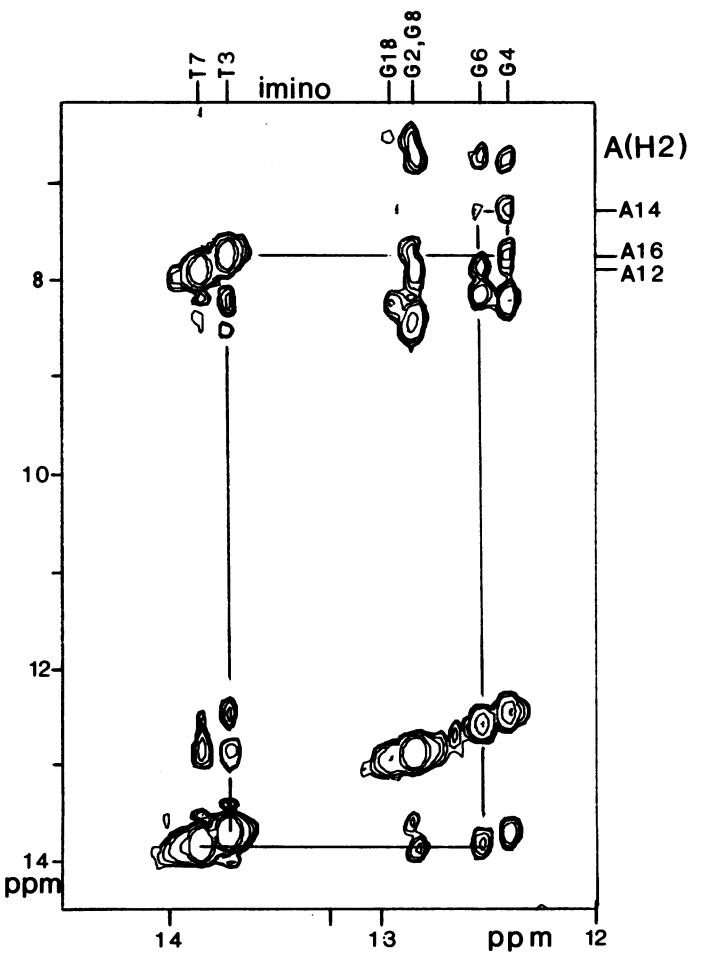

Fig. 2: Expanded contour plot of the region of imino, amino and base protons of the NOESY spectrum in H_2O at 1°C for τm=200ms.

Table I: Chemical shifts of non-exchangeable at 23°C and exchangeable protons at 1°C(+)

	H8/H6	H2(+)/ H5/CH_3	H1′	H2′	H2"	H3′	H4′	amino WC(+)/ amino nWC(+)	imino(+)
C1	7.62	5.87	5.73	2.02	2.42	4.70	4.06	6.57/8.22	
G2	7.98		6.00	2.68	2.78	4.98	4.34	*	12.88
T3	7.17	1.35	5.87	1.91	2.34	4.85	4.17		13.72
G4	7.94		6.12	2.63	2.68	4.99	4.37	*	12.44
dr5	-		3.81	2.02	2.02	4.75	4.05		
G6	8.01		6.04	2.65	2.80	4.92	4.37	*	12.58
T7	7.26	1.50	5.83	2.07	2.44	4.88	4.17		13.85
G8	7.86		5.92	2.58	2.68	4.96	4.33	*	12.88
C9	7.35	5.25	6.14	2.20	2.20	4.47	4.02	7.01/8.18	
G10	7.93		5.94	2.63	2.75	4.84	4.27	*	13.13
C11	7.45	5.43	5.64	2.09	2.41	4.88	4.17	6.80/8.33	
A12	8.28	7.86	6.19	2.73	2.86	5.02	4.42	*	
C13	7.24	5.32	5.69	1.96	2.37	4.79	4.16	6.69/8.11	
A14	7.97	7.23	6.02	2.35	2.56	4.85	4.17	*	
C15	7.37	5.47	5.22	1.98	2.26	4.77	4.24	6.77/8.18	
A16	8.27	7.70	6.20	2.72	2.83	5.01	4.42	*	
C17	7.27	5.35	5.66	1.86	2.26	4.78	4.12	6.59/8.46	
G18	7.87		6.13	2.35	2.60	4.65	4.16	*	12.99

(*) not observed.

from the WC and nWC proton of the cytidine and one corresponds to an AH2 seen also from the T imino resonances. The fourth cross peak corresponds to a non exchangeable proton not seen by the T iminos and must be of A14. The T imino resonance at 13.85 ppm gives two cross peaks with G imino resonances, at 12.58 and 12.88 ppm. This shows that the base pair corresponding to the T imino at 13.85 ppm is between the base pairs corresponding to these imino resonances. In the aromatic region the G imino resonance at 12.58 ppm shows two cross peaks at 6.69 and 8.12 ppm corresponding respectively to the nWC and WC cytidine amino protons. It shows a cross peak at 7.87 ppm corresponding to the AH2 resonance of the flanking A•T base pair and a weak cross peak at 7.2 ppm with the non exchangeable proton assigned to A14. This resonance at 7.2 ppm also shows a cross peak with the G imino resonance at 12.44 ppm. This shows clearly that the A14 is inside the helix between the base pairs corresponding to the G imino resonances at 12.44 and 12.58 ppm. This resonance at 7.2 ppm could be assigned to the A14(H8) proton, if the conformation of the base is *syn*, or to the A14(H2), if the conformation of A14 is *anti*. The G imino resonance at 12.44 ppm shows, apart from cross peaks to its cytidine WC and nWC amino protons, one to another AH2. Thus as shown in Fig. 2 we can follow the connectivities from one A•T base-se pair through a G•C, A14, another G•C to a second A•T base pair. Each

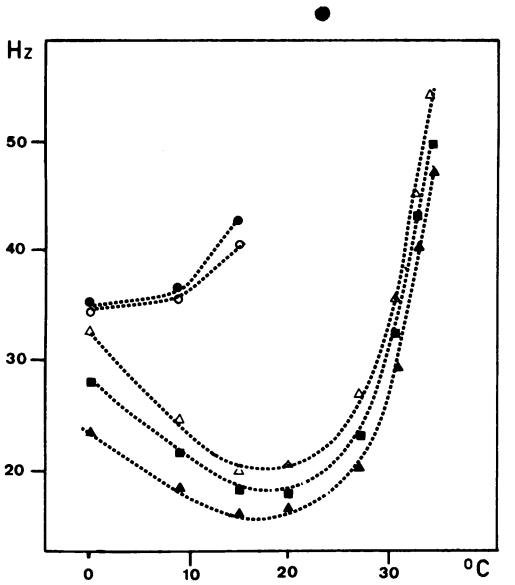

Fig. 3: Observed linewidths of the imino resonances of the duplex as a function of temperature for C1•G18 (O), C9•G10 (O), G2•C17 and G8•C11 (Δ), G4•C15 and G6•C13 (■), T3•A16 and T7•A12 (▲).

A•T shows a further connectivity with the almost coincident G imino protons at 12.99 ppm. Since the sequence has pseudo symmetry we cannot, however, determine the polarity of the chain from these connectivities alone.

Two 1D experiments were carried out to complete the assignement. The resonance of the terminal base pair at 12.99 ppm was presaturated for 0.5 s. It gives NOEs to its own cytidine WC amino proton at 8.22 ppm and to another one at 8.46 ppm. This latter was also observed in Fig. 2 from the T imino resonance at 13.7 ppm. This gives the complete assignment, except that being symmetric from the point of view of the imino resonances the direction is unknown. Presaturation of the other terminal resonance at 13.13 ppm showed that its nWC cytidine amino resonance is at 7.02 ppm. Presaturation of this resonance gave a strong NOE to a cytidine H5 resonance at 5.25 ppm which is assigned to the C9(H5) (see below). The observed chemical shifts are given in Table I.

We have recorded spectra of the duplex in H_2O as a function of temperature in order to measure the imino resonance linewidths and chemical shifts. The imino resonances move slowly to high field as the temperature is raised. The imino resonances of the terminal base pairs broaden and disap-

pear at lower temperature than the others due to rapid imino proton exchange with solvent via fraying. For all the other resonances the evolution of the linebroadening is very similar. The resonances decrease in linewidth as the temperature is raised to 20°C due to the decrease in viscosity. Above this temperature the base pairs melt out simultaneously, Fig. 3.

In order to investigate the effect of the abasic site upon the opening rate of the different base pairs, we have measured the imino proton lifetimes at 25°C. We have recently developped a method for measurement of proton exchange rates with solvent wich does not require independent determination of the dipolar contribution to T_1 (19). In the open limited case, the imino protons will exchange with solvent each time a base pair opens. We first checked if this was the case at 25°C, 10mM phosphate and pH 7.6. If the system is not in the open limited case, raising the pH should influence the imino proton linewidths and lifetimes. Experiments carried out at pH 8.0 show only differences which are within the experimental error, except for the terminal base pairs. We conclude that at pH 7.6 exchange is open limited for the non terminal base pairs.

The first part of the experiment involves measuring the transfer of magnetization upon continuous saturation of the H_2O resonance and comparing with the spectra without saturation. As expected, imino resonances of the penultimate base pairs are strongly reduced in intensity via fraying. The second part of the experiment involves measuring the selective spin lattice relaxation time T_1 in the presence of H_2O saturation. These two measurements provide both the dipolar contribution to T_1 and the imino proton lifetime τ_m in the closed state.

The results are given in Table II. The presence of the abasic site does not induce any major specific destabilisation of the adjacent base pairs. The absolute value of the lifetimes of the imino base pairs are in the range 200-500 ms and are comparable to those observed in other oligonucleotides duplexes.

NOESY in D_2O: assignment of non exchangeable protons

In order to assign the resonances of the non exchangeable base pro-

Table II: Life times of imino protons (in ms)

C	G	T	G	dr	G	T	G	C
G	C	A	C	A	C	A	C	G
	490	240	330		475	350	490	

tons H5, H6, H8 and sugar protons H1′, H2′, H2", H3′ and H4′, we have recorded NOESY, COSY and D2Q spectra of the duplex in D_2O at 23°C.We first recorded a NOESY in D_2O with a 300 ms mixing time. The cross peaks found in a NOESY spectrum correlate the chemical shifts of nuclei while cross relaxation occurs during the mixing time and thus are indicative of the proximity of the nuclei involved.

The most convenient starting point for the sequential assignment of resonances is from analysis of the H6/H8-H1′ region of the NOESY spectrum. The general principles and strategy for the assignment of proton spectra of oligonucleotides by NOESY have been described in detail (24-27)

The six strong cross peaks (x in Fig. 4) correspond to six doublets in the region between 5 and 6 ppm of the 1D resolution enhanced spectrum and can thus be assigned to the H5-H6 connectivities of the six cytidine residues. At 7.93 ppm we observe two cross peaks, one of them (B) corresponding to a base proton CH5 inter-residue interaction, the other, at 5.94 ppm, to the H1′ intra-residue interaction. The resonance at 7.93 ppm can be assigned to G10 which is the only 5′ terminal G. The H1′ resonance at 5.94 ppm gives

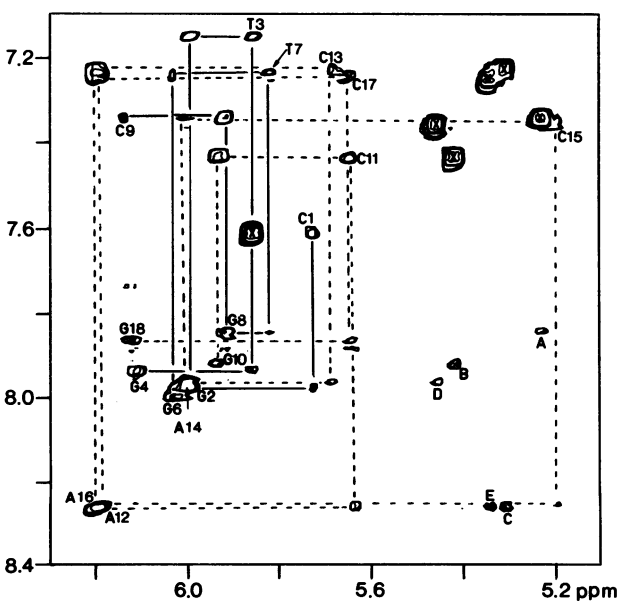

Fig. 4: Expanded NOESY contour plot of the region H6/H8-H1′/H5 of the duplex in D_2O at 23°C. The NOE connectivities are represented by (- - -) broken and (-----) continuous lines for strand A and B, respectively.

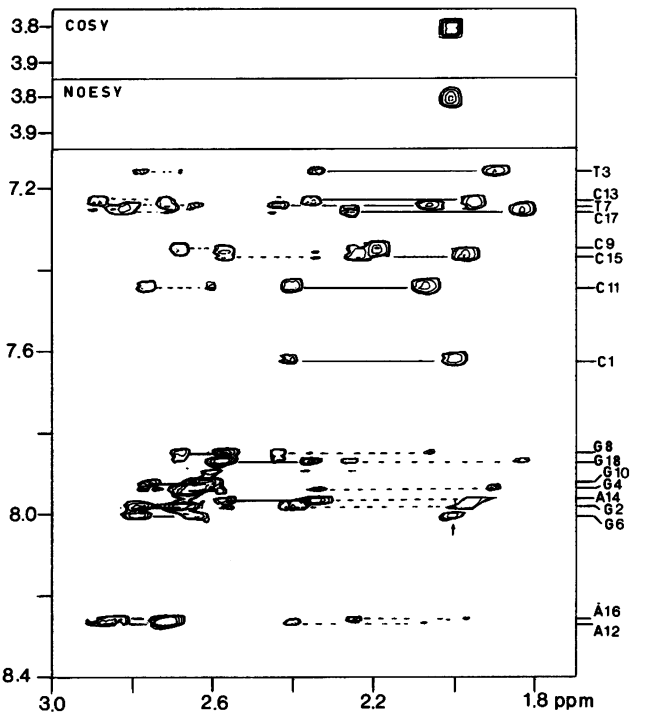

Fig. 5: Expanded contour plot of (a) the NOESY H6/H8-H2′/H2" region, (b) the NOESY H2′/H2"-(3.8-3.9ppm) region and (c) the COSY H2′/H2"-(3.8-3.9ppm) region of the duplex in D_2O at 1°C. The NOE connectivities are represented by broken (- - -) and continuous lines (-----) for inter and intra-residue connectivities, respectively.

a cross peak with a base proton at 7.45 ppm and can be assigned to C11(H6). At 7.45 ppm we observe also a H1′ cross peak at 5.64 ppm due to C11(H1′). At 5.64 ppm the ambiguity arising from the two possible connectivities is easily resolved by examination of the H8/H6-H2′/H2" region, Fig. 5. The sequential connectivities can be followed in both Figs 4 and 5 through the non base paired A14 to G18. We observe that the cross peak from the A14(H8) to its anomeric proton is normal in intensity and that the same is true for the intra and inter-residue cross peaks in the H2′/H2" region. Also the non exchangeable resonance of A14 observed in Fig. 2, which is at 7.27 ppm at 23°C, does not give rise to any cross peak in Fig. 4. We can thus conclude that A14 is in the anti conformation and that the resonance observed at 7.2 ppm in Fig. 2 corresponds to the H2 proton of A14. The connectivities for

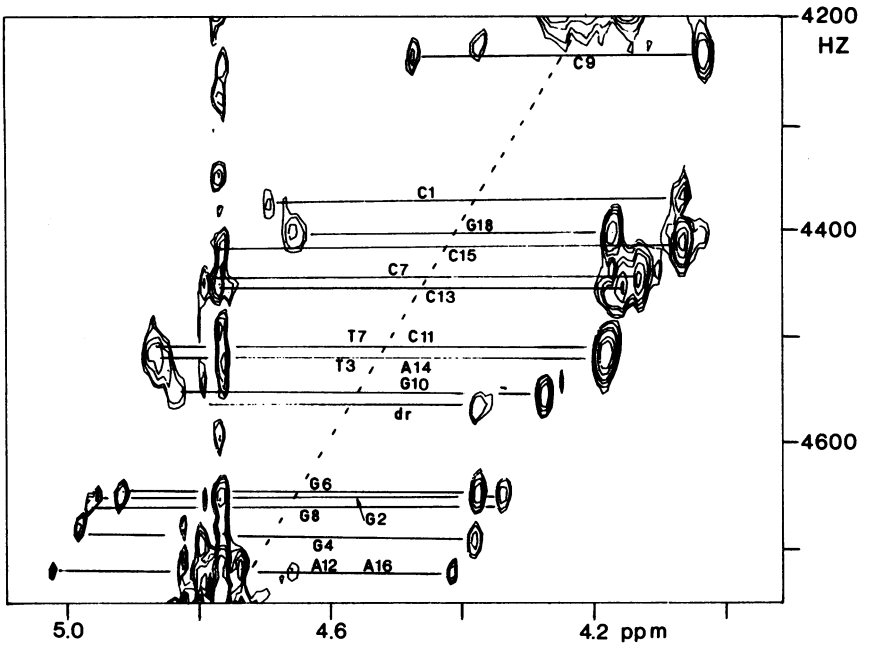

Fig. 6: Contour plot of the H3′/H4′ region of the 2D double quantum spectrum of the duplex at 23°C.

the other strand can be followed in Fig. 4 from C1 to G4, where the chain is broken, and from G6 to C9.

The G6(H8) resonance at 8.01 ppm gives rise to three cross peaks, two for the H2′ and H2" intraresidue interaction and another at 2.02 ppm which must be from the abasic site. In the COSY spectrum the resonance at 2.02 ppm gives a strong cross peak with another at 3.81 ppm which is also found in the NOESY spectrum in a region where there are no other cross peaks, Fig. 5. From These observations we can assign the 2.02 ppm resonance to the H2′/H2" and the 3.81 ppm resonance to the H1′/H1" of the deoxyribose without a base which must lie inside the helix.

The assignment of the H3′ protons requires the use of both COSY and NOESY type experiments. We followed the connectivities between H2′ and H3′ for all the sugars of the duplex. The assignment of the H4′ sugar protons was not possible on the basis of NOESY spectra, because in the region of the H4′ protons we also find some of the H5′ protons. The additional information given by the COSY spectrum was not sufficient. We therefore used a double quantum spectrum which gave the assignment of all the H4′ protons, Fig. 6.

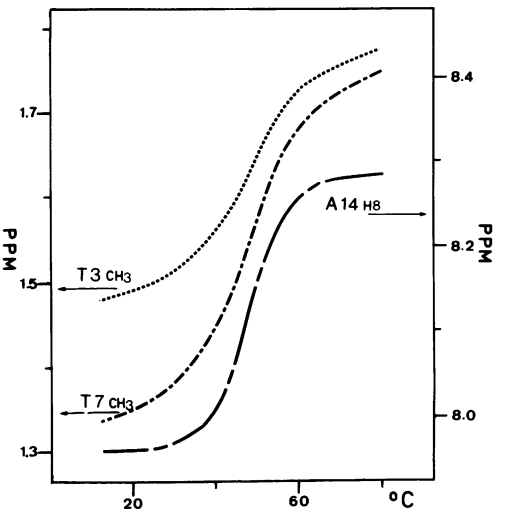

Fig. 7: Chemical shifts as a function of the temperature for T7(CH_3), T3(CH_3) and A14(H8).

Table 1 gives the observed chemical shifts for H5, H6, H8 base protons and H1′, H2′, H2", H3′, H4′ sugar protons of the duplex.

Tm Measurements

In order to compare the melting behaviour of the non hydrogen bonded

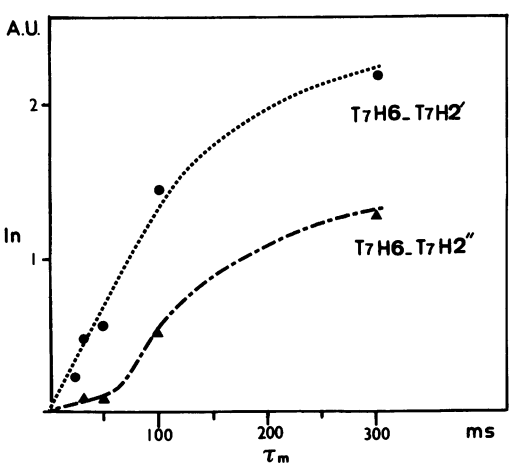

Fig. 8: Normalized magnitude of the NOE as a function of the mixing time for T7H(6)-T7(H2′) and T7(H6)-T7(H2") at 23°C.

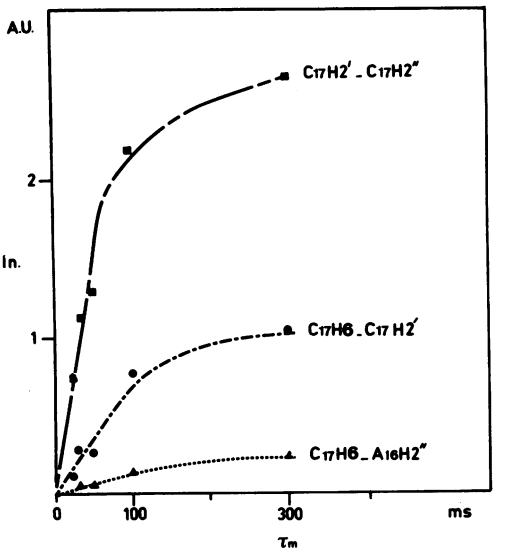

Fig. 9: Normalized magnitude of the NOE as a function of the mixing time for C17(H2')-C17(H2"), C17(H6)-C17(H2') and C17(H6)-A16(H2") at 23°C.

A14 with the A•T pairs, we followed the chemical shifts of A14(H8), T3(CH_3) and T7(CH_3) as a function of the temperature, Fig. 7. The curves show a typical sigmoid profile which corresponds to the double strand-single strand transition. We used the Tm to characterise these transitions. At the precision of the measurement, we observed for all three resonances the same Tm of 50±1°C.

Interproton distances

In order to determine the structure of the duplex, and especially in the region of the abasic site, we carried out a series of NOESY experiments. It is possible to evaluate interproton distances by estimating the slope of the build-up curve of the NOE between two nearby protons as a function of mixing time.

In Fig. 8 the intra residue NOE as a function of the mixing time for two pairs of protons, H6-H2' and H6-H2", are shown: there are clearly two different types of curves. The H6-H2' intraresidue NOE is a linear function of the mixing time below 70 ms. The H6-H2" intraresidue interaction gives a characteristic profile corresponding to a contribution from indirect interaction. In this case, the NOE is a linear function of the mixing time below 50 ms. For mixing times between 50 and 100 ms the rapid increase of the NOE is explained by contribution from spin diffusion. For both interactions the

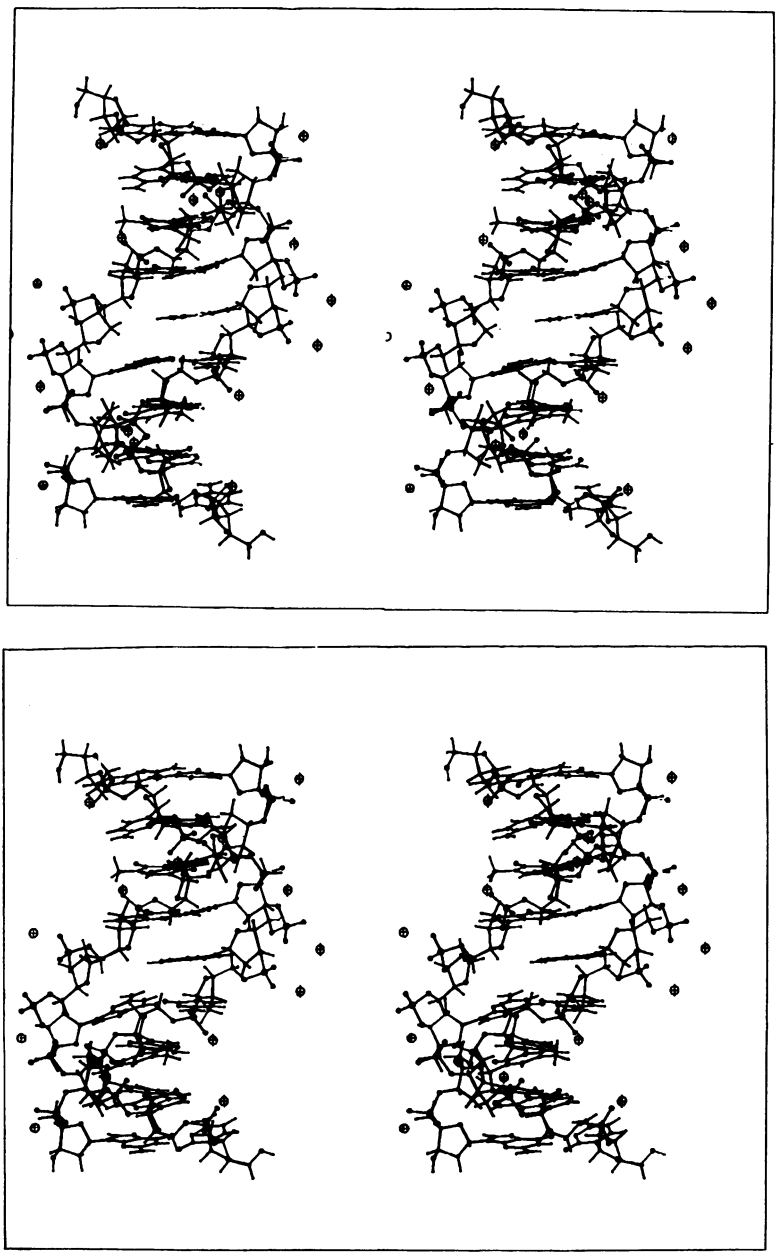

Fig. 10: Stereo views of structures S1 (top) and S2 (bottom) viewed from the minor groove.

Table III: Experimental (±10 %) and fitted proton-proton distances (in A) in the central region of the duplex.

	intra-residue		inter-residue	
	H1′->H2"	H6(H8)->H2′	H6(H8)->H2"	H6(H8)->H1′
T3	2.4	2.2		
	2.42	2.27		
G4	2.5	2.3	1.9	3.3
	2.44	2.56	2.16	3.53
dr5				
G6	2.6	2.2	2.2	3.9
	2.41	2.29	2.22	3.74
T7	2.4	2.3	2.3	3.1
	2.41	2.35	2.37	3.39
A12	2.5	2.4		
	2.41	2.35		
C13	2.5	2.3	2.3	3.5
	2.40	2.41	2.27	3.61
A14	2.4	2.2	2.1	3.9
	2.42	2.50	2.29	3.87
C15	2.7	2.2	2.0	3.9
	2.41	2.22	2.18	3.75
A16	2.5	2.4	2.2	3.5
	2.41	2.34	2.24	3.43

Top row: experimentally determined from NMR; bottom row: fitted distances after energy refinement.

NOE is a linear function of the mixing time below 50 ms. In this time domain the magnitude of the NOE, which corresponds to the dipolar contribution, is proportional to the inverse of the sixth power of the interproton distance.

Each interproton distance measurement requires the choice of a reference. This question leads to consideration of two different problems, the knowledge of certain distances, known or fixed, and the correlation time for the reference pair of protons. Two short distance direct interactions are extremely useful in determining DNA conformations. These are the intraresidue base H8/H6-H2′ interactions and the interresidue H8/H6-H2" interactions. It would appear that the NOEs for these two types of interaction have been interpreted using either (a) the fixed distance H2′-H2" NOE or (b) the cytidine H5-H6 NOE. Both assume the same correlation time for the intra and interresidue interaction, for which the interproton distance is 2.2±0.1A for a B form DNA (28-35).

We observe, however, that for this oligonucleotide, as for several others, this is not the case. Fig. 9 shows the NOE build up curves for C17(H6)-C17(H2′), C17(H6)-A16(H2") and C17(H2′)-C17(H2"). The first two show

Table IV: Comparison of the parameters of the refined structures S1 and S2.

Structure:	S1	S2
Energy (kcal)	-686.7	-695.7
Fit to NMR data: $\Sigma(d_{ij}-r_{ij})^2/r_{ij}$	0.82	0.44
Minor groove width:		
average distance	10.1	8.4
least distance separating the phosphorous atoms on opposite strands across the minor groove (S0=10.0 A)	9.9	8.0
Overall compaction (length of S0 = 28A)	0	-1
Pseudorotation angle of dr5	96	-4

initial slopes different by a factor of five despite having the same interproton distance in B DNA. While we observe that the fixed distance H2′-H2" NOE can be used to calibrate the intraresidue interaction, it would give rise to an error of 30% in the distance if used to calibrate the interresidue interaction. The relative ratios observed in Fig. 9 are independent of the dinucleotide pair in the helix. We have thus adopted a different strategy for determining interproton distances. The pattern of cross peaks observed in Figs.4 and 5 shows that the helix adopts a right handed B form conformation. This is confirmed, in so far as the sugar conformations are concerned, by the NOEs observed between the base H8 or H6 protons and the H2′ or H3′ protons of the same residue at mixing times < 50 ms. For an A type, C3′ endo sugar conformation, the base proton to H2′ and H3′ proton distances are very similar and we would expect that the NOE cross peak volumes would be similar. For a sugar conformation which is predominantly C2′ endo we would expect that the cross peak volume ratios, base proton-H2′ with respect to base proton-H3′, will be in the range 1:5 to 1:15. We observe for the non base paired A16 that this ratio is high, at least 1:15. For all other residues, except the 3′ terminal bases, the ratio is 1:ca.10, whereas for the 3′ terminal residues it is much smaller.

We observe that outside the central trinucleotide for a given type of proton-proton interaction the cross peak volumes at mixing times < 50ms are very similar except for the terminal residues. The same is true for the initial slopes of the NOE versus τ_m curves. We have therefore used these in conjunction with known standard B form interproton distances to calibrate

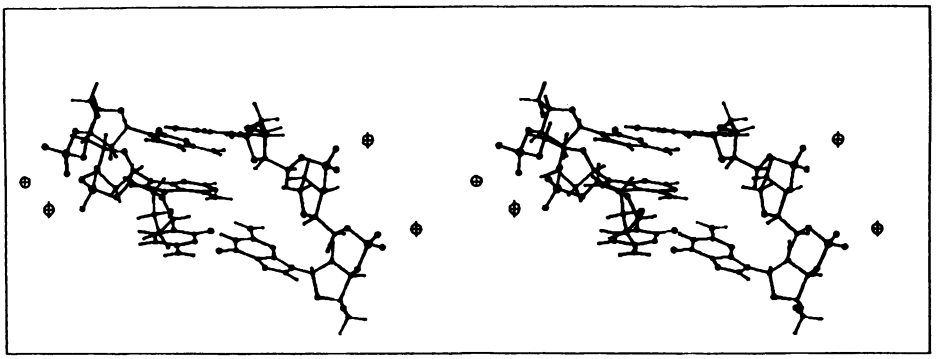

Fig. 11: Stereo view of the central part of structure S2 viewed from the major groove.

the NOE build up curves for the central part of the helix. We use the same type of interaction, e.g. H8-H2′, in the reference part to calculate distance for this interaction in the central part. In this way we can take into account variations in correlation time for each proton-proton vector. The desired distance is given simply by:

$$r_{ij} = r_{ref} \cdot (I_{ij} / I_{ref})^{1/6}$$

Using this strategy we have been able to calculate a set of interproton distances in the region of the abasic site, which are given in Table III. Given that only a limited number of degrees of freedom are available in double stranded DNA this is sufficient to define a time averaged structure.

DISCUSSION

The NOESY spectrum in H_2O, Fig. 2, shows that the A14 lies inside the helix. The aromatic proton of A14, which gives an NOE with the adjacent imino protons, but not with an anomeric proton, Fig. 4, must be assigned to A14(H2). The non hydrogen bonded A14 must therefore adopt the anti conformation. We have located all the resonances, except H5′/5", of the abasic site and the observed interresidue NOEs show that it must lie within the helix. As both the H1′/1" and H2′/2" resonances are coincident we cannot define the sugar conformation.

Qualitatively the absence of one base does not induce a major change from a normal B form DNA. The NOE build up curves for the central part of the helix confirm this. Indeed the calculated interproton distances show remarkably little variation from standard B DNA distances.

Both computed structures S1 and S2, Fig. 10, fit well the NMR data,

Table III, and are energetically close to each other, Table IV. They are both characterized by similar changes about the apyrimidinic site with the joint displacement of the central adenine and of the sugar on the opposite strand (dr5) towards the centre of the helix by about 0.5 A. Nevertheless, S1 is much closer to the Arnott energy minimized structure S0, than is S2. Table IV shows the following differences. The structure S2 is more compact than S1 and S0. The overall length is shorter, its minor groove is narrower, it is slightly more twisted. The sugar dr5 in S1 has kept the O4′ endo conformation that is found in S0 and that is characteristic of a pyrimidine sugar in a B double stranded DNA. In contrast, the sugar dr5 ring is C2′ exo as in a A type conformation in S2. In S1 the sugar dr5 is oriented radially and points towards the centre of the helix. When the base is absent, the atom C1′ may be supposed to more free. If C1′ can rotate around the axis C2′-O4′, then the sugar dr5 flips between O4′ endo and C2′ exo. A view of the central part of structure S2 seen from the major groove is shown in Fig. 11. In reality the conformation of the oligonucleotide may be described by a family of structures of which S1 and S2 are the limiting structures.

Loss of a base of DNA, generating an abasic site, significantly reduces helix stability (13). While a reduction in Tm is observed this instability is not localized to the abasic site. Interestingly we found that the A residue opposite the abasic site has the same Tm as the A residues in A•T base pairs two residues away in the same duplex. The oligonucleotide appears to undergo the helix to coil transition cooperatively, and does not unravel from the abasic site outward.

The geometry of the A residue opposite the abasic site is very close to the position it would assume in a normal A•T base pair. We have not yet examined the structure and dynamics of other bases opposite the abasic site, however we suggest that differences in polymerase insertion frequency might be related to deviation from normal base-paired geometry. If the incoming dNTP opposite the abasic site has a preferred orientation different from the normal geometry, or if it is relatively free to move, the efficiency of phosphate backbone condensation and base incorporation may be reduced. This could potentialy explain why differences in polymerase insertion frequencies at the abasic site are determined more by Vmax than Km (12). we are currently investigating the structures of oligonucleotides containing other bases opposite the abasic lesion.

Acknowledgement

We are most grateful to Mme. Dutreix for access to the Lexidata system. Work in Los Angeles was supported by grants GM 33863 and GM 21422 from the National Institutes of Health. L.S. was supported by NRSA 2T32CA09320-04 from the National Cancer Institute.

[3]Laboratoire de Physico-chimie Macromoléculaire, Institut Gustave Roussy, 94800 Villejuif, France

REFERENCES

1) Lindahl, T. & Nyberg, B. (1972) Biochemistry 11, 3610-3618
2) Lindahl, T. & Karlström, O. (1973) Biochemistry 12, 5151-5154
3) Lawley, P.D. & Brookes, P. (1963) Biochem. J. 89, 127-138
4) Lindahl, T. (1982) Ann. Rev. Biochem. 51, 61-87
5) Lindahl, T. (1979) Prog. Nucleic acids Res. Mol. Biol. 22, 135-192
6) Richards, R.G., Sowers L.C., Laszlo, J. & Sedgwick, W.D. (1984) Adv. Enzyme Reg.22, 157-185
7) Friedberg, E.C., Bonura, T., Radany, E.H. & Love, J.D. (1981) in The Enzymes 14, 251-279
8) Lockhart, M.L., Deutch, J.F., Yamaura, I., Cavalieri, L.F. & Rosenberg, B.H. (1982) Chem-Biol. Interact. 42, 85-95
9) Schaaper, R.M., Kunkel, T.A. & Loeb, L.A. (1983) Proc. Natl. Acad. Sc. U. S. 80, 487-491
10) Sagher, D. & Strauss, B. (1983) Biochemistry 22, 4518-4526
11) Kunkel, T.A. (1984) Proc. Natl. Acad. Sci. USA 81, 1494-1498
12) Randall, S.K., Eritja, R., Kaplan, B.E., Petruska, J. & Goodman, M.F. (1987) J. Biol. Chem. 262, 6864-6870
13) Millican, T.A., Mock, G.A., Cahuncy, M.A., Patel, P.T., Eaton, M.A.W, Grunning, J., Cutbush, S.D., Neidle, S. & Mann, J. (1984) Nucleic Acids Res. 12, 7435-7453
14) Gait, M.J. (1984) "Oligonucleotide synthesis, a practical approach", IRL Press, Oxford
15) Eritja, R., Walker, P.A., Randall, S.K., Goodman, M.F. & Kaplan, B.E. (1987) Nucleosides and Nucleotides 6, 803-814
16) Bodenhausen, G., Kogler, H. & Ernst, R.R. (1984) J. Magn. Res. 58, 370-388
17) Braunschweiler, L., Bodenhausen, G. & Ernst, R.R. (1983) Mol. Phys. 48, 535-560
18) Clore, G.M., Kimber, B.J. & Gronenborn, A.M. (1983) J. Magn. Res. 54, 170-173
19) Quignard, E., Buu, B. & Fazakerley, G.V. (1986) J. Magn. Res. 67, 342-345
20) Weiner, P.K. & Kollman, P.A. (1981) J. Comp. Chem. 2, 287-303
21) Weiner, S.J., Kollman, P.A., Case, D.A., Singh, U.C., Ghio, C., Alagona, G., Profeta, S., Jr. & Weiner, P.K. (1984) J. Am. Chem. Soc. 106, 765-784
22) Gelin, B. & Karplus, M. (1977) Proc. Natl. Acad. Sci. USA 81, 801-805
23) Arnott, S., Campbell-Smith, P. & Chandresekharan, P. (1976) CRC Handbook of Biochemistry Vol.2, 411-41
24) Hare, D.R., Wemmer, D.E., Chou, S.H., Drobny, G. & Reid, B.R. (1983) J. Mol. Biol. 181, 319-336

25) Feigon, J., Leupin, W., Denny, W.A. & Kearns, D.R. (1983) Biochemistry 22, 5943-5951
26) Fréchet, D., Cheng, D.M., Kan, L.S. & Ts'o, P.O.P. (1983) Biochemistry 22, 5194-5200
27) Scheek, R.R., Boelens, R., Russo, N., van Boom, J.H. & Kaptein, R. (1984) Biochemistry 23, 1371-1376
28) Gronenborn, A.M., Clore, G.M. & Kimber, B.J. (1984) Biochem. J. 221, 723-736
29) Hogan, M.E. & Jardetzky, O. (1980) Biochemistry 19, 3460-3468
30) Bolton, P.H. & James, T.L. (1979) J. Phys. Chem. 83, 3359-3367
31) Kollmann, P.A., Keepers, J.W. & Weiner, P.K. (1982) Biopolymers 21, 2345-2376
32) Levitt, M. (1983) Cold Spring Harbor Symp. Quant. Biol. 47, 251-262
33) Tidor, B., Irikura, K.K., Brooks, B.R. & Karplus, M. (1983) J. Biomol. Struct. Dyn. 1, 231-252
34) Hare, D.R. & Reid, B.R. (1986) Biochemistry 25, 5341-5350
35) Hare, D.R., Shapiro, L. & Patel, D.J. (1986) Biochemistry 25, 7456-7464